$C_6H_5(CH_2)_2$), 90147-73-2; **7a** (R = *i*-Pr, $R^3$ = $C_6H_5(CH_2)_2$), 127931-46-8; **7b** (R = Et, $R^3$ = *p*-$ClC_6H_4$), 40394-88-5; **7b** (R = Et, $R^3$ *p*-$MeOC_6H_4$), 132566-33-7; **7b** (R = Et, $R^3$ = $CH_3(CH_2)_{10}$), 132566-34-8; **7b** (R = Et, $R^3$ = $C_6H_5(CH_2)_2$), 132566-35-9; **7b** (R = Et, $R^3$ = $C_6H_5$), 40394-84-1; **8**, 13965-03-2; **9**, 132566-21-3; **10**, 68391-84-4; **12**, 104750-69-8; **13**, 132566-32-6; **14**, 10199-34-5; *cis*-**15a**, 132566-24-6; *trans*-**15a**, 132566-36-0; **15b**, 132566-25-7; **15c**, 132566-26-8; **16a**, 132566-27-9; **16b**, 132566-29-1; **16c**, 132566-30-4; **17a**, 132566-28-0; **17b**, 53647-50-0; **17c**, 132566-31-5; **18**, 12012-95-2; **19**, 60068-19-1; **20**, 127931-49-1; **21**, 41798-91-8; $C_6H_5COCl$, 98-88-4; $(C_6H_5CO)_2O$, 93-97-0; $C_6H_5COBr$, 618-32-6; *p*-$ClC_6H_4COCl$, 122-01-0; *p*-$MeOC_6H_4COCl$, 100-07-2; (*E*)-$C_6H_5CH$=$CHCOCl$, 17082-09-6; $CH_3(CH_2)_{10}COCl$, 112-16-3; $C_6H_5(CH_2)_2COCl$, 645-45-4; $CH_3CH_2COCl$, 79-03-8; 1-$C_{10}H_7COCl$, 879-18-5; 2-$MeC_6H_4COCl$, 933-88-0; 3-$MeC_6H_4COCl$, 1711-06-4; $(CH_3)_2C$=$CHCOCl$, 3350-78-5; $C_6H_5CO(CH_2)_2COC_{10}H_7$-1, 127931-48-0; *p*-$MeOC_6H_4CO(CH_2)_2COC_6H_5$, 60755-22-8; *p*-$MeOC_6H_4CO(CH_2)_2COC_6H_4$-*o*-Me, 127931-50-4; *p*-$MeOC_6H_4CO$-$(CH_2)_2COC_6H_4$-*p*-Cl, 67756-16-5; $CH_3CH_2COCH(CH_3)CH_2CO$-$C_6H_5$, 121862-34-8; $PdCl_2$, 7047-10-1; $PdCl_2$(*o*-$Tol_3P)_2$, 40691-33-6; $Pd(Ph_3P)_4$, 14221-01-3; $Pd_2(dba)_3$·$CHCl_3$, 52522-40-4; *p*-$MeOC_6H_4CH_2COOEt$, 14062-18-1; 1-((trimethylsilyl)oxy)-1-phenylcyclopropane, 38858-73-0; 1-((trimethylsilyl)oxy)-1-(2-furyl)cyclopropane, 132566-22-4; 1-((trimethylsilyl)oxy)bicyclo-[4.1.0]heptane, 38858-74-1; 2-thenoyl chloride, 5271-67-0; 1-(2-furyl)-4-(3-methylphenyl)butane-1,4-dione, 127931-51-5; 2-[2-(1-naphthyl)-2-oxoethyl]cyclohexanone, 127931-52-6; 2-[2-(2-thienyl)-2-oxoethyl]cyclohexanone, 54669-95-3; 1-(2-thienyl)-3-methylhexane-1,4-dione, 132566-23-5; 1-((trimethylsilyl)oxy)-1-ethyl-2-methylcyclopropane, 113777-09-6.

# Structural Requirements for Glyme Catalysis in Butylaminolysis of Aryl Acetates in Chlorobenzene. Identification of $-OCH_2CH_2OCH_2CH_2OCH_2CH_2O-$ as the Optimal Subunit for Catalysis

John C. Hogan and Richard D. Gandour*

*Department of Chemistry, Louisiana State University, Baton Rouge, Louisiana 70803-1804*

*Received September 25, 1990*

The catalytic behavior of linear (open-chain) polyethers (glymes) in butylaminolysis of 4-nitrophenyl acetate carried out in chlorobenzene has been reexamined (*J. Am. Chem. Soc.* **1980**, *102*, 2865–2866). The observation of a break in a plot of the catalytic rate constant vs chain length of catalyst indicates that four oxygens in a $-OCH_2CH_2OCH_2CH_2OCH_2CH_2O-$ subunit are necessary for optimal catalysis. The break, occurring at four oxygens in the profile (corresponds to triglyme), has been verified by a Hammett analysis, which employed four additional aryl acetates (3-chlorophenyl, 3-bromophenyl, 3-cyanophenyl, and 4-cyanophenyl). This break was missed in a previous study (*J. Am. Chem. Soc.* **1980**, *102*, 2865–2866) because differing amounts of impurities in the glymes increased the experimental scatter of the data. The Hammett study supports the conclusions of others that breakdown of the zwitterionic tetrahedral intermediate is rate-limiting. The break in the polyether plot implies a specific structure for a glyme–zwitterionic tetrahedral intermediate complex, which contains an ammonium ion that hydrogen bonds to the ether oxygens.

## Introduction

In 1980, we demonstrated[1] that conformational flexibility enhances the catalytic power of glymes in the butylaminolysis of 4-nitrophenyl acetate conducted in chlorobenzene. We showed that glyme catalysis of this reaction exhibits an *inverse macrocyclic effect*;[2] i.e., open-chain polyethers, GLM(*n*), are better catalysts than macrocyclic polyethers. Our desire to understand the mechanism of this host–guest interaction between a catalyst and transition structure prompted a more detailed examination, which we report herein.

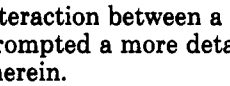

GLM(n)

Ester aminolysis carried out in nonpolar media[3–5] proceeds via the rate-determining breakdown of a tetrahedral intermediate, $T^{\pm}$. The rate expression, eq 1, indicates a termolecular transition structure. Base catalysis of the

$$k_{obs} = k_0[\text{amine}]^2 + k_{cat}[\text{amine}][\text{catalyst}] \quad (1)$$

reaction involves[5–7] a hydrogen-bonded complex, presumably between the catalyst and the ammonium ion part of $T^{\pm}$. Scheme I illustrates a minimal mechanism. Formation of the catalyst·$T^{\pm}$ complex can occur by two paths. Breakdown of the complex most likely limits the rate.

Glyme catalysis of this aminolysis improves[1] as the number of basic oxygen atoms per catalyst molecule increases, which is the expected behavior if complexation assists in the rate-determining breakdown of $T^{\pm}$. Complexation by polyether bases to an acidic site (i.e., the ammonium region of $T^{\pm}$) should improve with the number

**Table I. Melting and Boiling Points of Aryl Acetates**

| substituent | mp or bp (Torr), °C | lit. bp (Torr) or mp, °C | lit. ref |
|---|---|---|---|
| 3-chloro | 70.5 (2) | 105–109 (15–16) | 8 |
| 3-bromo | 86.5 (2) | 142 (34) | 9 |
| 3-cyano | 60.0–60.5 | 58 | 9 |
| 4-cyano | 57.0–58.0 | 56–57 | 8 |
| 4-nitro | 78.0–79.5 | 79 | 9 |

(1) Hogan, J. C.; Gandour, R. D. *J. Am. Chem. Soc.* **1980**, *102*, 2865–2866.
(2) Cabbiness, D. K.; Margerum, D. W. *J. Am. Chem. Soc.* **1969**, *91*, 6540–6541.
(3) Menger, F. M.; Smith, J. H. *J. Am. Chem. Soc.* **1972**, *94*, 3824–3829.
(4) Menger, F. M.; Vitale, A. C. *J. Am. Chem. Soc.* **1973**, *95*, 4931–4934.
(5) Nagy, O. B.; Reuliaux, V.; Bertrand, N.; Van Der Mensbrugghe, A.; Leseul, J.; Nagy, J. B. *Bull. Soc. Chim. Belg.* **1985**, *94*, 1055–1074.
(6) Su, C.-W.; Watson, J. W. *J. Am. Chem. Soc.* **1974**, *96*, 1854–1857.
(7) Jencks, W. P. *Chem. Rev.* **1985**, *85*, 511–527.

0022-3263/91/1956-2821$02.50/0 

**Scheme I**

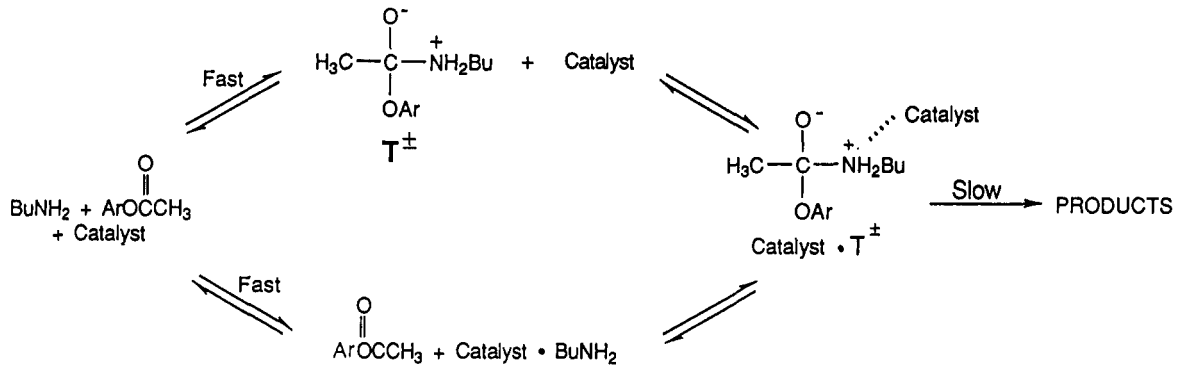


of complexing oxygens per polyether molecule up to a certain number of oxygens. We present evidence that four oxygens in a $-OCH_2CH_2OCH_2CH_2OCH_2CH_2O-$ subunit are necessary for optimal catalysis, and we expand the conclusions of the preliminary report in 1980. A Hammett study of butylaminolysis of a series of aryl acetates provides further data for speculation about the mechanism of catalysis.

## Experimental Section

**Materials.** Chlorobenzene (Alfa/Mortion Thiokol) was used as received. Butylamine (Aldrich) was purified by fractional distillation from metallic sodium and stored under argon. Aryl acetate esters (Table I) were prepared by dissolving the corresponding phenols in excess pyridine, adding excess acetic anhydride, and stirring the resulting reaction mixtures for at least 8 h, followed by cold aqueous workup and simple (bulb-to-bulb Kugelrohr) distillation or recrystallization from hexane. The melting points or boiling points agreed with literature values[8,9] (see Table I). Monoglyme, diglyme, triglyme, and tetraglyme (Aldrich) were purified by bulb-to-bulb distillation from metallic sodium. Hexaglyme and heptaglyme (Parish Chemical) were purified in the same fashion. These purified polyethers all showed single spots by silica gel TLC (10% 2-propanol/hexanes).

**Pentaglyme, GLM(6).** To 2.00 g (7.93 mmol) of pentaethylene glycol monomethyl ether (Parish Chemical) was added 4 g of sodium hydroxide (Holcross Chemical, technical grade) and 20 mL of dry dioxane (freshly distilled from molten sodium). This mixture was stirred at reflux for 1 h, after which 2.00 g (15.9 mmol) of dimethyl sulfate (Aldrich) was added dropwise, producing a vigorous reaction. The reaction mixture was refluxed for 1 h, cooled to room temperature, and partitioned between 50 mL of dichloromethane and 30 mL of water. The resulting organic layer was washed twice with 50 mL each of distilled water, dried with magnesium sulfate, concentrated by rotary evaporation, and stirred over molten sodium metal for 1 h. The excess sodium was then removed from the resulting brown gelatinous suspension, which was bulb-to-bulb (Kugelrohr) distilled under 1.0 Torr pressure in a 150 °C oven (lit.[10] bp 153–155 °C (3 Torr)), yielding approximately 0.5 g of a dark brown solid and 1.44 g (68.2%) of a water-white oil, whose $^1H$ NMR and silica gel TLC were consistent with pure pentaglyme ($R_f$ 0.37, 1:9 2-propanol/hexanes): $^1H$ NMR ($CCl_4$, 60 MHz) $\delta$ 3.29 (s, 6 H), 3.32–3.67 (m, 20 H).

**Octaglyme, GLM(9).** Tetraethylene glycol (18.0 g, 92.7 mmol, Aldrich) was mixed with 100 mL of pyridine (Reilly Chemical) in an ice bath. Methanesulfonyl chloride (44.4 g, 388 mmol, Aldrich) was slowly added to this mixture with swirling. The resulting exothermic reaction was kept below 25 °C. The reaction mixture was stored at −20 °C overnight and then poured onto 100 g of cracked ice and extracted with 200 mL of dichloromethane. The resulting organic layer was washed with 200 mL of cold 6 N HCl followed by 200 mL of saturated sodium bicarbonate. The organic layer was then dried with magnesium sulfate, filtered, concentrated, and allowed to lose residual solvents under reduced pressure (1.0 Torr) overnight, yielding 32.5 g (92.8 mmol, 100%) of a bright orange oil whose $^1H$ NMR was consistent with pure tetraethylene glycol dimesylate.

Metallic sodium ribbon (20 g, Aldrich) was pressed into a reaction vessel containing 100 mL of tetrahydrofuran (QO Chemical) that was freshly distilled from sodium ribbon. A solution of 25.0 g of diethylene glycol monomethyl ether (Aldrich) and 75 mL of tetrahydrofuran was added to the reaction vessel over a period of 30 min with stirring. The resulting reaction mixture was refluxed 2 h and then cooled in an ice bath. A solution of the tetraethylene glycol dimesylate in 75 mL of tetrahydrofuran was added to the reaction vessel over a period of 30 min. The resulting reaction mixture was warmed to room temperature and then refluxed for 2 h. The liquid portion was decanted from the remaining sodium ribbon and added, with swirling, to 20 mL of water, yielding a light yellow liquid above a white precipitate. The liquid layer was filtered, dried ($MgSO_4$), filtered again, and concentrated by rotary evaporation, yielding ~40 g of a dark yellow oil. A total of 8 mL of clear material was collected from the distillation of the oil at reduced pressure (0.07 Torr), bp 32–120 °C. The remaining oil was distilled at reduced pressure three times after stirring over molten sodium for 2 h each time. The final distillation yielded 10.8 g (28.7%) of a clear oil, bp 190 °C (0.1 Torr). A 1-gram portion of this material was chromatographed on a 20 × 20 cm glass-backed 60-Å silica gel TLC plate (1-mm layer thickness, E-M Science) with 10% 2-propanol/hexanes yielding two fractions: $R_f$ 0.26, ~85% (visual density); $R_f$ 0.39, ~15% (visual density). The lower fraction ($R_f$ 0.26) was scraped away from the plate and extracted three times with acetone (20 mL each time). The combined extracts were filtered, concentrated, and distilled from molten sodium, yielding 0.432 g of clear oil, bp 190 °C (0.1 Torr) (lit.[11] bp 215–218 °C (0.45 Torr)), whose $^1H$ NMR and TLC were consistent with pure octaglyme ($R_f$ 0.25, 1:9 (v/v) 2-propanol/hexanes): $^1H$ NMR ($CCl_4$, 60 MHz) $\delta$ 3.28 (s, 6 H), 3.35–3.64 (m, 32 H).

**Table II. Experimental Kinetics Conditions Used in Aminolysis of Aryl Acetates**

| substituent | wavelength monitored, nm | [butylamine], M | $10^5$[ester], M |
|---|---|---|---|
| 3-chloro | 293 | 0.15 | 130 |
| 3-bromo | 293 | 0.15 | 120 |
| 3-cyano | 297.5 | 0.15 | 25 |
| 4-cyano | 293 | 0.06 | 120 |
| 4-nitro | 320 | 0.04 | 8.1 |

**Kinetics.** Reactions were carried out by weighing the polyether catalysts in 1 cm × 3 mL square cuvettes, pipetting 3 mL of butylamine/chlorobenzene stock solution (see Table II for butylamine stock concentrations) into the same cuvettes, thermostating the resulting solutions for 0.5 h at 25 °C, injecting 30–40 μL of ester/chlorobenzene solution into each cuvette (see Table II for ester concentrations), stoppering the cuvettes, shaking, and

(8) Van Etten, R. L.; Sebastian, J. F.; Clowes, G. A.; Bender, M. L. *J. Am. Chem. Soc.* **1967**, *89*, 3242–3253.
(9) Nishioka, T.; Fugita, T.; Kitamura, K.; Nakajima, M. *J. Org. Chem.* **1975**, *40*, 2520–2525.
(10) Chan, L. L.; Wong, K. H.; Smid, J. *J. Am. Chem. Soc.* **1970**, *92*, 1955–1963.
(11) Yanagida, S.; Takahashi, K.; Okahara, M. *Bull. Chem. Soc. Jpn.* **1978**, *51*, 1294–1299.

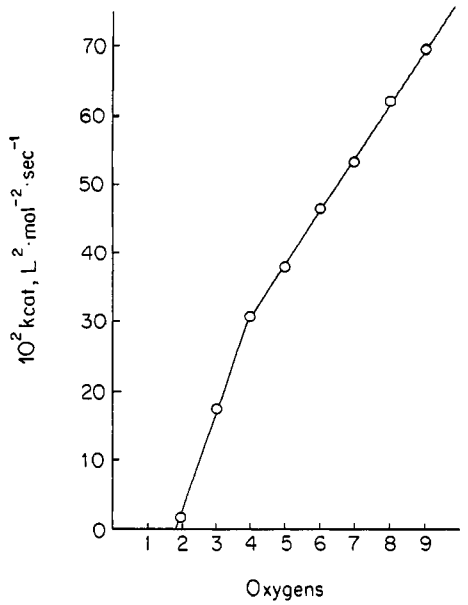


**Figure 1.** Plot of catalytic rate constant, $k_{cat}$, for butylaminolysis of 4-nitrophenyl acetate vs number of oxygens in the linear polyether catalyst molecule.

collecting absorbance vs time data at fixed wavelength (see Table II for wavelengths used). The appearance of substituted phenol (product) was followed at the wavelength selected. Isosbestic points were obtained for all esters studied under the reaction conditions employed in these aminolyses. Absorbance data were measured by a Cary 118C spectrophotometer with a five-cell timed sample changer. The data thus collected were timed, formatted, and tagged with sample numbers (1–5) by a Varian 310 data interface. The resulting time absorbance sample data were stored on an 8-in. floppy diskette by a Data General Nova 3 minicomputer. Interleved data from five separate simultaneously reacting samples were separated and stored by this system. Pseudo-first-order rate constants (excess butylamine) were obtained by analyzing the diskette data with a modified version of the program LSKINI developed by Detar,[12] which fits absorbance vs time data to the equation $A = A_\infty + (A_0 - A_\infty)\exp(-k_{obs}t)$, where $A_\infty$, $A_0 - A_\infty$, and $k_{obs}$ are iteratively optimized to achieve the best possible least-squares fit. LSKINI was executed on an IBM model 370/3033 or 370/3081 mainframe computer system. Catalysis kinetics were run with five different catalyst concentrations in five sample cuvettes reacting simultaneously. This protocol was triplicated for each catalyst/ester combination studied. All samples in a simultaneous run were made from the same butylamine stock solution. Uncatalyzed studies were done by running five samples of the same butylamine stock solution simultaneously after adding 30–40 μL of ester and quintuplicating this protocol by use of different butylamine concentrations. Nearly 500 $k_{obs}$s were measured (see supplementary material). Catalytic rate constants were determined by fitting $k_{obs}$ to eq 1. Values of $k_0$ for different esters were obtained from the slopes of plots of $k_{obs}$/[amine] vs [amine] from noncatalytic experiments in which five different amine concentrations were studied. Values of $k_{cat}$ for different polyether catalysts with a given ester were obtained from the slopes of plots of $k_{obs}$/[amine] vs [catalyst]. Kinetic slopes and Hammett slopes were calculated with a simple linear least-squares program running on a Texas Instruments TI99/4A home computer.

## Results

**Redetermination of Catalytic Power vs Oxygen Number Profile.** All linear polyethers, GLM($n$), larger than diglyme ($n$ = 3) used to determine our original $k_{cat}$ vs oxygen per catalyst profile in 1980[1] were obtained from Parish Chemical Co. and used without further purification. Subsequent analysis indicated that only two of these polyethers, GLM(7) and GLM(8), could be purified sufficiently by distillation from sodium metal to appear pure by TLC. Consequently, GLM(6) and GLM(9) were synthesized. GLM(5) and smaller polyethers were obtained from Aldrich. Our new $k_{cat}$ vs oxygens per catalyst profile was therefore redetermined with use of glymes that were TLC pure (see Experimental Section for details).

The resulting $k_{cat}$ vs oxygen per catalyst profile (see Figure 1 and Table III) for butylaminolysis of 4-nitrophenyl acetate shows a distinct downward break at four oxygens. (We missed this break previously because of differing amounts of impurities in the glymes, which increased the apparent experimental scatter of the data points). This breakpoint occurs in butylaminolysis of the other aryl esters (see the following text).

A clearer picture of this saturation phenomenon is a plot of $k_{cat}$/oxygens per catalyst vs the number of oxygens in the catalyst (Figure 2). Catalysis increases as the number

**Table III. Catalytic Power ($k_{cat}$) vs Oxygen Number Profile for Polyethers Monoglyme through Octaglyme**

| catalyst | oxygens | $10^2k_{cat}$, M$^{-2}$ s$^{-1}$ | $10^3k_{cat}$/oxy, M$^{-2}$ s$^{-1}$ oxy$^{-1}$ |
|---|---|---|---|
| GLM(2) | 2 | 1.78 ± 0.03 | 8.9 ± 0.2 |
| GLM(3) | 3 | 17.4 ± 0.2 | 58 ±1 |
| GLM(4) | 4 | 30.8 ± 0.3 | 77 ± 1 |
| GLM(5) | 5 | 38.1 ± 0.3 | 76 ± 1 |
| GLM(6) | 6 | 46.4 ± 0.3 | 77.3 ± 0.5 |
| GLM(7) | 7 | 53.5 ± 0.2 | 76.4 ± 0.3 |
| GLM(8) | 8 | 62.2 ± 0.8 | 78 ± 1 |
| GLM(9) | 9 | 69.7 ± 0.5 | 77.4 ± 0.6 |

**Table IV. Uncatalyzed Hammett Data from Substituted Phenyl Acetate Butylaminolysis Kinetics**

| substituent | σ | $10^3k_0$, M$^{-2}$ s$^{-1}$ | log $k_0$ |
|---|---|---|---|
| 3-chloro | 0.37 | 1.08 ± 0.05 | −2.97 ± 0.04 |
| 3-bromo | 0.39 | 1.15 ± 0.03 | −2.94 ± 0.02 |
| 3-cyano | 0.68 | 4.7 ± 0.1 | −2.32 ± 0.02 |
| 4-cyano | 1.00 | 25.5 ± 0.4 | −1.59 ± 0.01 |
| 4-nitro | 1.27 | 65.1 ± 0.8[a] | −1.19 ± 0.01[a] |

[a] Obtained from an analysis of the data presented in ref 19.

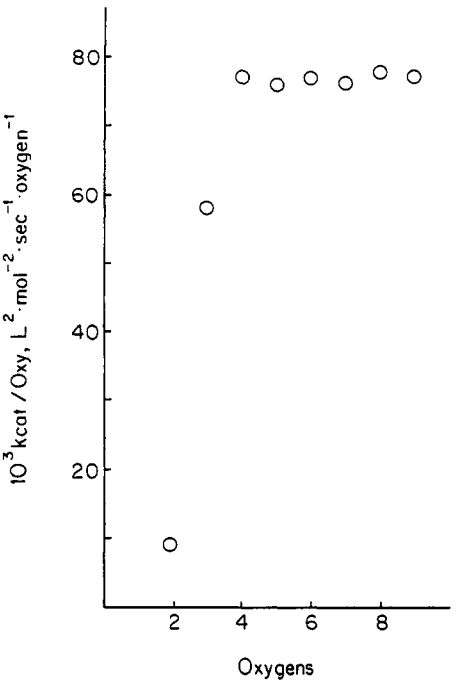


**Figure 2.** Plot of the per oxygen catalytic rate constant, $k_{cat}$/oxy, vs the number of oxygens per catalyst molecule.

(12) Detar, D. F. *Computer Programs for Chemistry. I.*; W. A. Benjamin: New York, 1968.
(13) Jaffé, H. H. *Chem. Rev.* **1953**, *53*, 191–261.

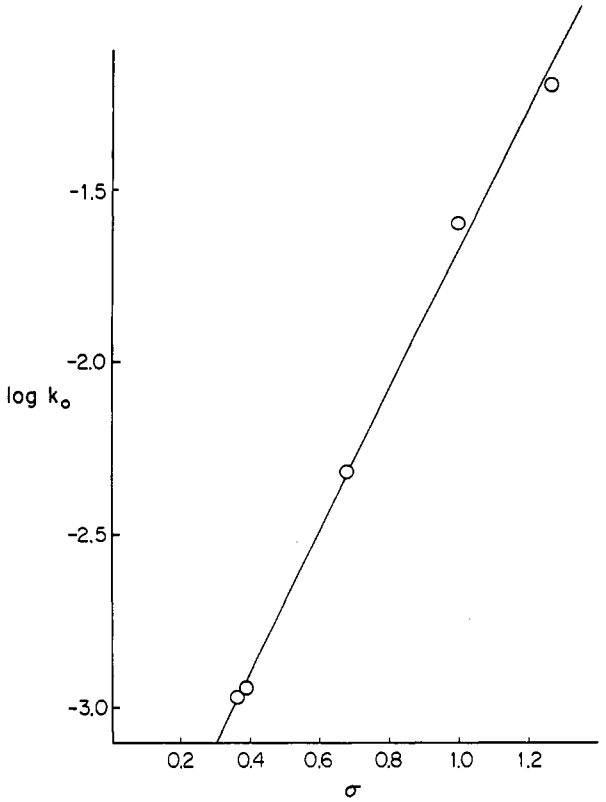


**Figure 3.** Uncatalyzed Hammett plot for the butylaminolysis of aryl acetates in chlorobenzene.

**Table V. Catalyzed and Uncatalyzed Hammett ρ Values Obtained from Aminolysis Rate Constant Correlations[a]**

| catalyst | oxygens | ρ | $10^3 k_{cat}$/oxy, $M^{-2}$ $s^{-1}$ $oxy^{-1}$ |
|---|---|---|---|
| none | | 2.04 ± 0.08 | |
| GLM(2) | 2 | 1.94 ± 0.09 | 8.9 ± 0.2 |
| GLM(3) | 3 | 2.16 ± 0.05 | 58 ± 1 |
| GLM(4) | 4 | 2.5 ± 0.1 | 77 ± 1 |
| GLM(5) | 5 | 2.4 ± 0.1 | 76 ± 1 |
| GLM(9) | 9 | 2.4 ± 0.1 | 77.4 ± 0.6 |

[a] The catalytic ρ values show the same trend as per oxygen catalytic powers.

of oxygens increases. The profile then levels off at four oxygens, and successive oxygens only contribute to the catalysis in a statistical manner.

**Hammett Study of Uncatalyzed Butylaminolysis.** Table IV lists values of $k_o$ for butylaminolysis of aryl acetates along with the substituent constants. A Hammett plot is shown in Figure 3. We use $\sigma^-$ instead of $\sigma_p$ for 4-cyano and 4-nitro[13] to achieve the best correlation. The ρ value (2.04) sets the reference to which the polyether catalysts are compared (Table V). This value indicates considerable negative-charge transfer to the aryloxy group. Values of this magnitude are typical in aprotic solvents.[3,5]

**Hammett Study of Glyme-Catalyzed Butylaminolysis.** Table VI lists log $k_{cat}$ for butylaminolysis of the aryl acetates catalyzed by GLM($n$), $n$ = 2–5 and 9. Figure 4 shows the corresponding Hammett plots. ρ values

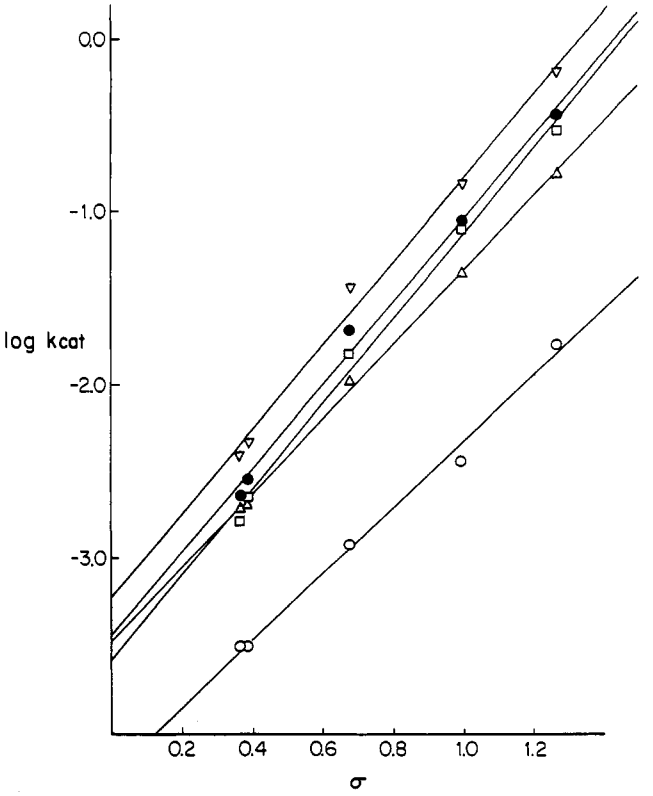


**Figure 4.** Catalyzed Hammett plots corresponding to data in Table VI: (○) monoglyme (GLM(2)); (△) diglyme (GLM(3)); (□) triglyme (GLM(4)); (●) tetraglyme (GLM(5)); (▽) octaglyme (GLM(9)).

are tabulated in Table V. The reaction catalyzed by GLM(2) has a ρ value slightly smaller than the uncatalyzed reaction. ρ increases for GLM(3) and again for GLM(4). ρ values for GLM(5) and for GLM(9) are identical, but slightly smaller than GLM(4). The error limits make these last three values indistinguishable. A plot of ρ vs oxygen number for these catalysts (Figure 5) resembles Figure 2.

## Discussion

**Interpretation of Break in Figure 2.** The break demonstrates that four oxygens in an $-OCH_2CH_2OCH_2CH_2OCH_2CH_2O-$ subunit of the catalyst form a binding site (presumably for the ammonium ion part of $T^{\pm}$) in the rate-limiting termolecular transition structure. Figure 2 indicates that glymes with four or more oxygens use only four oxygens to catalyze the butylaminolysis. A linear plot of the $k_{cat}$s for glymes with four or more oxygens intercepts the origin (intercept ± standard error is 0.008 ± 0.006 $L^2$ $mol^{-2}$ $s^{-1}$). This result shows that catalysis by glymes with four or more oxygens correlates with the effective concentration of four oxygen subunits, $-OCH_2CH_2OCH_2CH_2OCH_2CH_2O-$, in solution. The subunit concentration increases with both the molar concentration of and the number of oxygens in a glyme.

Okamoto and co-workers call this increase in catalysis with increase in chain length the *polymer cosolvent effect*.[14] They provide a thermodynamic expression in terms

**Table VI. log $k_{cat}$ Values Used in Hammett Correlations**

| catalyst | 3-chloro | 3-bromo | 3-cyano | 4-cyano | 4-nitro |
|---|---|---|---|---|---|
| none | −2.97 ± 0.04 | −2.94 ± 0.02 | −2.32 ± 0.02 | −1.59 ± 0.01 | −1.19 ± 0.01 |
| GLM(2) | −3.5 ± 0.2 | −3.5 ± 0.1 | −2.91 ± 0.03 | −2.42 ± 0.05 | −1.75 ± 0.01 |
| GLM(3) | −2.69 ± 0.04 | −2.68 ± 0.04 | −1.96 ± 0.02 | −1.325 ± 0.007 | −0.76 ± 0.01 |
| GLM(4) | −2.77 ± 0.05 | −2.63 ± 0.04 | −1.80 ± 0.02 | −1.09 ± 0.01 | −0.511 ± 0.008 |
| GLM(5) | −2.62 ± 0.03 | −2.53 ± 0.04 | −1.67 ± 0.01 | −1.03 ± 0.02 | −0.419 ± 0.006 |
| GLM(9) | −2.39 ± 0.09 | −2.31 ± 0.07 | −1.42 ± 0.01 | −0.82 ± 0.01 | −0.157 ± 0.006 |

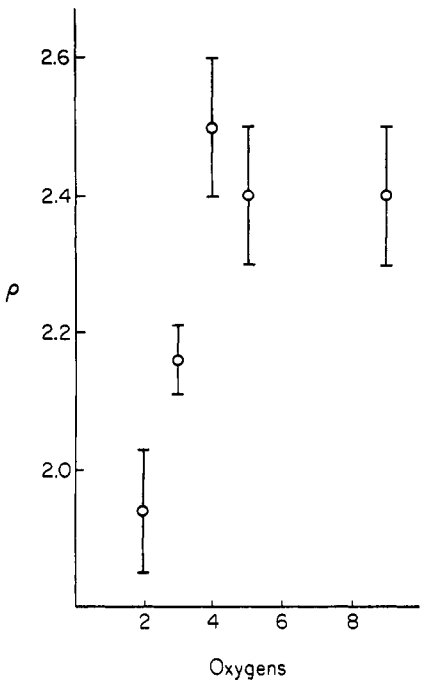


**Figure 5.** Plot of catalyzed ($k_{cat}$) Hammett $\rho$ values vs oxygens per molecule of linear polyether catalysts. $\rho$ values were obtained from the slopes of the plots in Figure 4. Error bars were derived from standard errors associated with linear least-squares fits to the data.

of chain length, pair-interaction parameters, and volume fraction of oligomer cosolvent. They show from our earlier data[1] that the catalytic constants of glymes with four or more oxygens are linearly related to their expression. Their approach implies that the catalytic power, on a molar basis, of long glymes should, in theory, increase linearly with chain length, provided that conformations of the catalyst do not create regions that are inaccessible to $T^{\pm}$.

**Interpretation of $\rho$ Values. 1. Magnitude.** Large positive values of $\rho$ indicate build up of electron density (negative charge) on the aryloxy moiety. The magnitude also depends on the nature of the solvent. Previous workers[3-5] interpret these large positive values as evidence for rate-determining breakdown of $T^{\pm}$ in aminolyses of aryl acetates and benzoates in aprotic solvents. We support this interpretation and offer additional evidence for rate-limiting breakdown of $T^{\pm}$ in butylaminolysis of aryl acetates catalyzed by glymes in chlorobenzene.

**2. $\rho$ vs Oxygens in Catalyst (Figure 5).** As the number of oxygens per glyme increases from two to four, $\rho$ increases from 1.94 to 2.5 (Table V). $\rho$ is constant for greater than four oxygens. As catalysis increases, $\rho$ increases then levels off (Figure 5). This behavior parallels the plot in Figure 2. The parallel behavior confirms that the glymes with four or more oxygens catalyze the butylaminolyses of these aryl acetates in a similar manner and that the $-OCH_2CH_2OCH_2CH_2OCH_2CH_2O-$ subunit is optimal for catalysis.

The increase in $\rho$ with increase in catalysis suggests that the breakdown of $T^{\pm}$ is rate-limiting. An energy vs reaction-progress diagram (Figure 6) illustrates this point. Glymes should complex to the ammonium ion part of $T^{\pm}$, the transition structure for breakdown, and the transition structure for formation when glyme preassociates with the nucleophile. This complexation stabilizes the intermediate state $T^{\pm}$, the transition state for breakdown of $T^{\pm}$, and to a lesser degree because of smaller positive charge, the

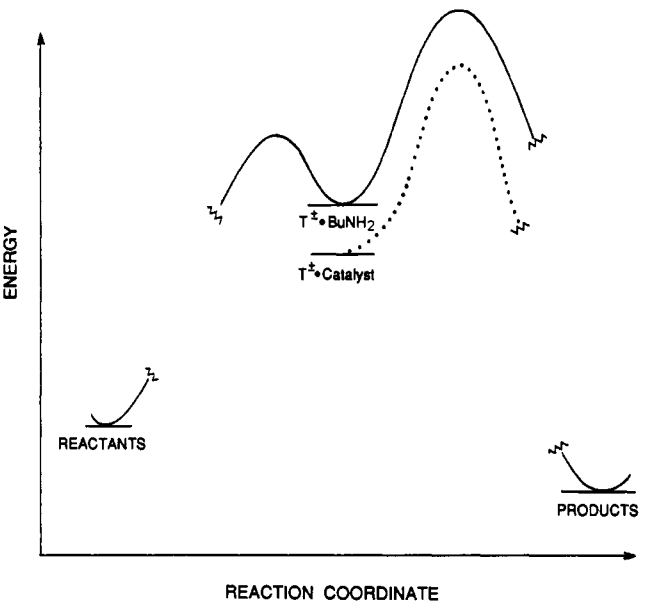


**Figure 6.** Reaction coordinate energy diagram for butylaminolysis of aryl acetates in chlorobenzene: solid curve, uncatalyzed path; hashed curve, catalyzed path.

transition state for formation of $T^{\pm}$. Stabilization of the intermediate state with respect to reactant or product produces a "later" transition state for breakdown and an "earlier" transition structure for formation. Increase in $\rho$ with increase in catalysis indicates that a later transition state is rate-limiting.

**Mechanism of Catalysis.** In a recent study of butylaminolyses of many esters in aprotic solvents, Nagy et al.[5] report excellent Brønsted relationships and endorse Su and Watson's[6] proposal that hydrogen bonding to the ammonium ion part of $T^{\pm}$ is more important than proton basicity for catalysis. The catalytic efficiency of the glymes in this reaction also supports the hydrogen-bonding proposal. Polyethers bind ammonium ions, and such binding is enhanced in aprotic solvents. In chlorobenzene, hydrogen-bond acceptors stabilize ammonium ions, which otherwise would not form. Stabilization of the ammonium ion part of $T^{\pm}$ in the transition state for breakdown produces catalysis.

Our Hammett data imply that the interaction of glymes with $T^{\pm}$ facilitates expulsion of the aryloxy group. An intramolecular 1,3-dipolar stabilization between the oxyanion and the ammonium ion must exist in uncomplexed $T^{\pm}$. A hydrogen bond acceptor that forms a complex with the ammonium ion part of $T^{\pm}$ must do so at the expense of breaking up this intramolecular dipolar stabilization. The negative charge would then be dispersed between the oxyanion and aryloxy group. An increase in $\rho$ measures the increase in negative charge on the aryloxy group. The net result is that hydrogen bonding to the ammonium ion part weakens the bond to the aryloxy group. As the binding of a glyme increases the "nudity"[15] of the charge on the oxyanion, the more readily the aryl oxide leaves.

What remains unclear is whether butylamine preferentially preassociates[16] with the glyme (or another butylamine molecule in the "uncatalyzed" mechanism) followed by attack of the resulting complex on the ester to form $T^{\pm}$ or, alternatively, butylamine attacks the ester to form uncomplexed $T^{\pm}$ followed by binding to glyme (Scheme I). The rate-determining transition structure occurs *after*

(14) Okamoto, A.; Hayashi, T.; Mita, I. *Polymer J.* **1983**, *15*, 423–427.

(15) Liotta, C. L.; Harris, H. P. *J. Am. Chem. Soc.* **1974**, *96*, 2250–2252.
(16) Jencks, W. P. *Acc. Chem. Res.* **1980**, *13*, 161–169.

the formation (by either alternative) of *complexed* $T^{\pm}$. How the product forms is also uncertain, but there are two likely possibilities. One is a stepwise process where complexed $T^{\pm}$ decomposes to a tight ion pair (aryloxide and complexed N-protonated amide)[17] followed by a proton transfer to give a phenol and the amide. The other, a concerted path, avoids the tight ion pair. In other words, glyme shuttles a proton[18] from the ammonium ion to the aryl oxide.

**Host-Guest Interaction.** The optimal catalysis by an $-OCH_2CH_2OCH_2CH_2OCH_2CH_2O-$ subunit implies a specific host-guest interaction between a glyme and the rate-limiting transition structure. We propose a complex, $CT^{\pm}$, in which four oxygens donate electron density to

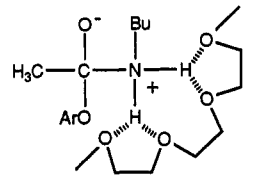


$CT^{\pm}$

stabilize both hydrogens of the ammonium ion part of $T^{\pm}$. Given the size of the $-{}^{+}NH_2-$ fragment, four oxygens are probably the maximum that can bind it. We offer that the guest transition structure organizes the host. This organization results in *transition-structure recognition* by the host. The imprint left by a transition structure in a flexible host reveals a part of the structure of the guest.

(17) Perrin, C. L. *Acc. Chem. Res.* **1989**, *22*, 268-275.
(18) We thank a reviewer of a previous version of this manuscript for this suggestion.

## Conclusions

Glymes catalyze butylaminolysis of aryl acetates in chlorobenzene by binding to the ammonium ion part of $T^{\pm}$ formed by attack of butylamine on the ester. The $-OCH_2CH_2OCH_2CH_2OCH_2CH_2O-$ subunit is optimal for this binding interaction. The binding interaction accelerates the breakdown of $T^{\pm}$ by weakening the bond to the aryloxy group as seen by an increase in $\rho$ with increasing catalysis. The relationship between catalysis and subunit structure suggests that the ammonium ion part of the transition structure is recognized by the catalyst. Studies are in progress to uncover the details of this recognition.

**Acknowledgment.** We thank Mr. Don Patterson for technical assistance and the Research Corporation for the initial support of this work. We dearly thank Mrs. Mary Jane Peters for her assistance and encouragement.

**Supplementary Material Available:** Observed rate constants for uncatalyzed and oligoglyme-catalyzed butylaminolysis of substituted phenylacetates at 25 °C in chlorobenzene (32 pages). Ordering information is given on any current masthead page.

# The Synthesis of 2,3,3a,4,5,7a-Hexahydro-1*H*-inden-1-ols by Intramolecular Diels-Alder Reactions of 1,3,8-Nonatrien-5-ols. Dependence of Product Stereochemistry on the Substitution Pattern

Alan P. Kozikowski and Werner Tückmantel*

*Mayo Clinic Jacksonville, Neurochemistry Research, 4500 San Pablo Road, Jacksonville, Florida 32224*

*Received July 16, 1990*

A short and efficient synthesis of the title compounds is described, starting from readily available $\alpha,\beta$-unsaturated carbonyl compounds **5** and $\beta,\gamma$-unsaturated ketones **4**. Their directed aldol condensation yields the unsaturated hydroxy ketones **6** which are dehydrated to the trienones **7**. Athough these fail to cyclize on heating, the intramolecular Diels-Alder reaction can be brought about after reduction or alkyllithium addition to the carbonyl group. Alkyl substitution in the positions 1, 2, 3, 5, and 7 has little influence on the ease and yield of cyclization, whereas a methyl group at C-4 hinders it considerably. The title compounds are obtained as mixtures of usually all four stereoisomers, of which one predominates (≥50%) in most cases. O-Alkylation in **8b** has little effect on the isomer distribution. The major isomer of the 6-bromo derivative forms a highly crystalline *p*-nitrobenzoate **27**, which permits stereochemical assignment through X-ray crystallography; for most other products assignments can be made by comparison and further evaluation of their $^1H$ NMR spectra. The results are discussed in terms of a simple transition state model. The intramolecular Diels-Alder reaction fails when the length of the tethering chain is reduced by one, or when the diene unit becomes part of a furan ring. Trienones **7** are sensitive to autoxidation, of which some products are described.

The intramolecular Diels-Alder reaction is a powerful tool of organic synthesis,[1] although stereoselectivity is often moderate. In the course of a larger synthetic project, we needed a simple and efficient access to 2,3,3a,4,5,7a-hexahydro-3,3-dimethyl-1*H*-inden-1-ol, **18b**. The relative stereochemistries at C-1/C-7a and C-3a/C-7a were not a major issue because C-1 would later be oxidized to the ketone and C-7a subjected to epimerization. It appeared therefore promising to procure **18b** by an intramolecular Diels-Alder ring closure of its open-chain isomer **17b**, the corresponding ketone **7b**, or protected derivatives thereof. While the preparation of the triene precursors may be cumbersome in other cases, **7b** ought to be accessible by dehydration of the aldol **6b**, and this in turn through directed aldol addition[2] of the kinetic enolate of the known[3]

(1) (a) Brieger, G.; Bennett, J. N. *Chem. Rev.* **1980**, *80*, 63. (b) Ciganek, E. *Org. React.* **1984**, *32*, 1. (c) Taber, D. F. *Intramolecular Diels-Alder and Alder Ene Reactions*; Springer: New York, 1984. (d) Fallis, A. G. *Can. J. Chem.* **1984**, *62*, 1831. (e) Salakhov, M. S.; Ismailov, S. A. *Russ. Chem. Rev.* **1986**, *55*, 1145. (f) Roush, W. R. *Advances in Cycloaddition*; Curran, D. P., Ed.; JAI Press: Greenwich, 1990; Vol. 2, pp 91-146.

0022-3263/91/1956-2826$02.50/0 